Journal of Applied Polymer Science

Selective Adsorption of Au^{3+} from Aqueous Solutions Using Persimmon Powder-Formaldehyde Resin

Feng Xie, Zaijun Fan, Qinglin Zhang, Zhengrong Luo
Key Laboratory of Horticultural Plant Biology (MOE), Huazhong Agricultural University, Wuhan 430070, China
Correspondence to: Z. R. Luo (E-mail: luozhr@mail.hzau.edu.cn)

ABSTRACT: A new adsorption resin has been developed by immobilizing persimmon powder with formaldehyde, and its adsorption properties to Au^{3+} were investigated in detail. The resin exhibited outstanding selective adsorption capacity towards Au^{3+} from acidic aqueous solutions (pH 2.0), which the equilibrium adsorption capacity was high up to 3025.20 mg g^{-1} at 323 K. The resin exhibited 100% adsorption of Au^{3+} within 8 h, and the experimental data were well fitted with the pseudo-first/second-order rate model. The adsorption isotherms could be well described by Freundlich equation. The column studies suggested that the resin was effective for the adsorption of Au^{3+} from aqueous solutions, and the loaded Au^{3+} could be easily desorbed by acidic thiourea solution. The adsorption of Au^{3+} was an endothermic reductive adsorption process. This suggested that the resin can be used as an active biosorbent for the recovery of Au^{3+} from aqueous environment. © 2013 Wiley Periodicals, Inc. J. Appl. Polym. Sci. 130: 3937–3946, 2013

KEYWORDS: adsorption; biopolymers and renewable polymers; resins; recycling

Received 3 October 2012; accepted 8 May 2013; Published online 3 July 2013
DOI: 10.1002/app.39521

INTRODUCTION

Nowadays, gold is widely used in electric and electronic devices due to its high chemical stability, fine ductility, and high conductivity. Obsolete electric and electronic devices (e-wastes) such as cellular phones, televisions, and computers contain larger amounts of gold than gold ores, which may be considered as secondary ore of gold. It was reported that cellular phones contain 200 g of gold per ton of scrap which was much higher than the content in gold ores, which was only 5–30 g of gold per ton of ore.[1] Due to natural gold resource is limited and nonrenewable, it is necessary to find ways to recycle gold from various wastes especially e-wastes to fulfill the increasing demand. Many alternatives have been reported for the effective recovery of gold from aqueous solutions such as precipitation, solvent extraction, reverse osmosis, electrodialysis, and adsorption. Among these methods, adsorption is promising for the gold recovery because it offers prominent advantages, especially can be applied for the water treatment at low concentrations. For this reason, numerous studies on the gold adsorption have been conducted so far using various adsorbents such as activated carbon,[2] minerals,[3] synthetic resin,[4,5] hydrogel,[6] nanocomposite,[7] and so on. Nevertheless, these adsorbents are not so effective (low capacity and/or poor selectivity) or have high cost. Therefore, the search for environmentally benign and low cost biosorbent materials for gold recovery is urgent. Since the last few years researches on biosorbents for gold recovery from aqueous solutions were concerned with tannin,[1] microorganism,[8,9] agricultural wastes,[10–12] algae,[13,14] polysaccharide,[15–17] and so on.

Tannin is one of the most abundant biomasses in nature, which is distributed in different parts of plants and trees such as roots, barks, seeds, and fruits. In general, tannin can be classified as hydrolysable tannin and condensed tannin according to different chemical structures and persimmon (*Diospyros kaki* Thunb.) tannin (PT) belongs to the condensed type. As shown in Figure 1, PT consists of four catechin compounds (catechin; catechin-3-gallate; gallocatechin; gallocatechin-3-gallate = 1 : 1 : 2 : 2), which connect in series and its average molecular weight is 1.38×10^4.[18] The B-rings of PT consist of a great majority of adjacent hydroxyl groups, which can react with metal ions. In addition, the presence of galloyl group that attached to part of C-rings can increase the number of adjacent hydroxyl groups that promote reactions of tannin with metal ions as well.[19] Some researchers have focused on the PT, especially on its application for gold recovery for the past few years.[20–25] Three waves of physiological drop of persimmon fruits may occur 5-80 days after full blossom each year. What is more, a large number of persimmon fruits are always thinned as redundant fruits for guaranteeing the quality of fruit in production practice. In addition, about 80% of persimmon fruits in China are used for

Additional Supporting Information may be found in the online version of this article.

Applied Polymer SCIENCE

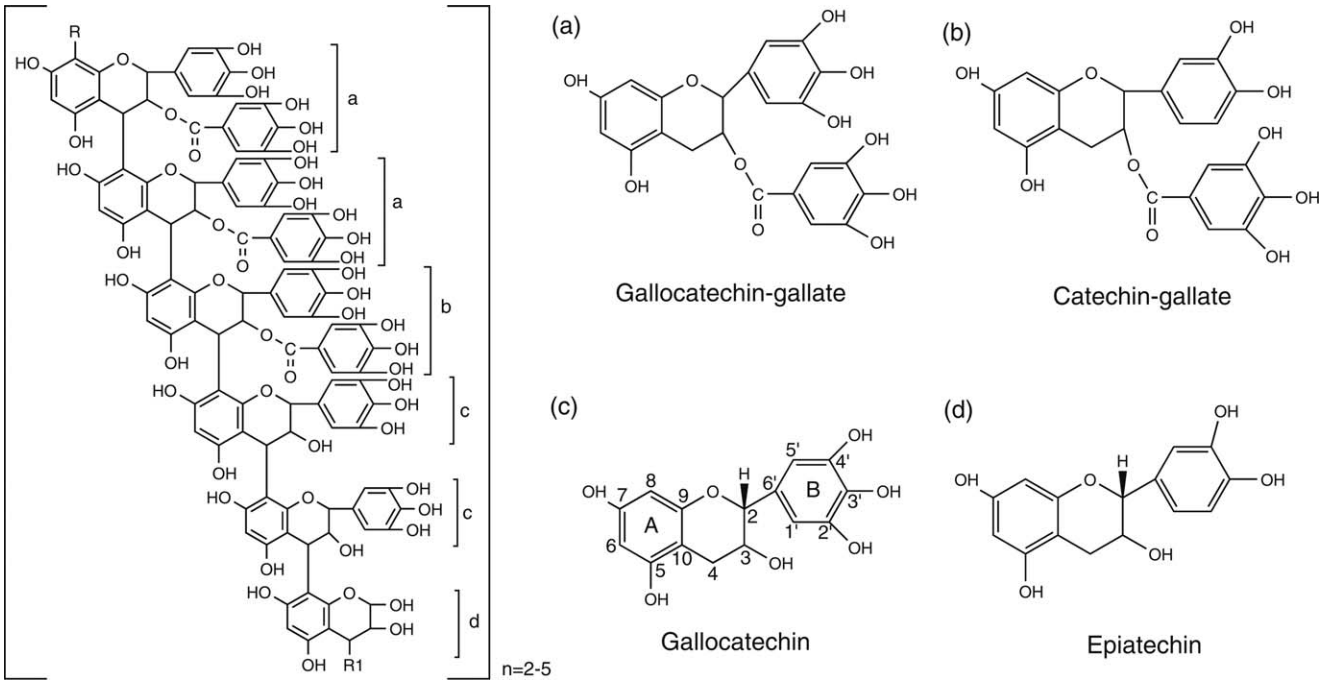

Figure 1. Chemical structure of persimmon tannin and related catechin compounds.

further processing, particularly to produce dried persimmon, which generate large amount of persimmon peel. These physiological drop fruits, artificial thinning fruits, and fruit peels produced in processing generate huge amount of persimmon waste. However, this persimmon waste contains abundant PT, which has high affinity to some specified metal ions such as Au^{3+}, and it is promising to prepare adsorbent from them.

Since PT is partly water-soluble, its application of adsorbent is limited. Therefore, it should be transformed into water insoluble matrix so as to overcome this problem. Formaldehyde is one of the most effective crosslinking agents for tannin.[1,26] The A-rings of tannin can react with formaldehyde due to their strong nucleophilicity, and the probable active-sites is C_6.[26] In this work, persimmon powder was immobilized by formaldehyde to prepare biosorbent for gold recovery from aqueous solutions and its adsorption behavior toward Au^{3+} was evaluated. Meanwhile, the application potential of this biosorbent for the recovery of Au^{3+} from actual industrial liquor had also been tested.

EXPERIMENTAL

Materials

A sample of dry persimmon powder was kindly donated by Huikun Agriculture Product (Gongcheng, China), which was prepared following this method: first, persimmon waste was squeezed and then the generated juice was freeze-dried. The content of PT in the powder was determined to be about 30% with the Folin–Ciocalteu method.[27] Gold adsorption experiments were carried out with fresh solutions that were prepared from stock solution of chloroauric acid tetrahydrate ($AuCl_3 \cdot HCl \cdot 4H_2O$). The pH of solutions was adjusted with diluted HCl or NaOH solution.

Preparation of the Persimmon Powder-Formaldehyde Resin

The adsorption resin was prepared referring to the method proposed by Nakano et al.[28] The persimmon powder (30 g) was dissolved in 65 mL of NaOH solution (0.25 mol L^{-1}) at room temperature, which was followed by addition of 6 mL of formaldehyde (37 wt %) as a crosslinking reagent. After resination at 353 K for 12 h, the product was filtered, then crushed and grinded into powder and followed by washing successively with deionized water and HNO_3 solution (0.05 mol L^{-1}) to remove unreacted substances, and finally rinsed with deionized water. Thus, the obtained adsorbent was dried for 24 h at 338 K, which was named as persimmon powder-formaldehyde resin (PPF resin) and used for carrying out all adsorption experiments.

Batch Adsorption Studies

Batch experiments for Au^{3+} were carried out in sealed conical flasks at a constant temperature shaking for 24 h at a speed of 200 r min^{-1}. The effect of pH on the adsorption of Au^{3+} was conducted at 303 K by mixing 15 mg of PPF resin with 50 mL of Au^{3+} solution (150 mg L^{-1}) over the pH range of 2.0–6.0. In kinetic studies, 15 mg of PPF resin was mixed with 50 mL of Au^{3+} solution (100 mg L^{-1}) at 303, 313, and 323 K, respectively, the pH of the solution was adjusted around 2.0 and samples were withdrawn at desired time intervals. In isotherm experiments, 15 mg of PPF resin was added to 50 mL of Au^{3+} solution with varied initial concentrations (150-350 mg L^{-1}) at 293, 303, and 313 K, respectively, the pH of each solution was adjusted around 2.0. All the adsorption experiments were replicated three times and the errors were found to be within 5%.

Column Experiment: Loading and Elution

A continuous-mode column experiment was carried out at room temperature (298 ± 5 K) using a transparent glass column

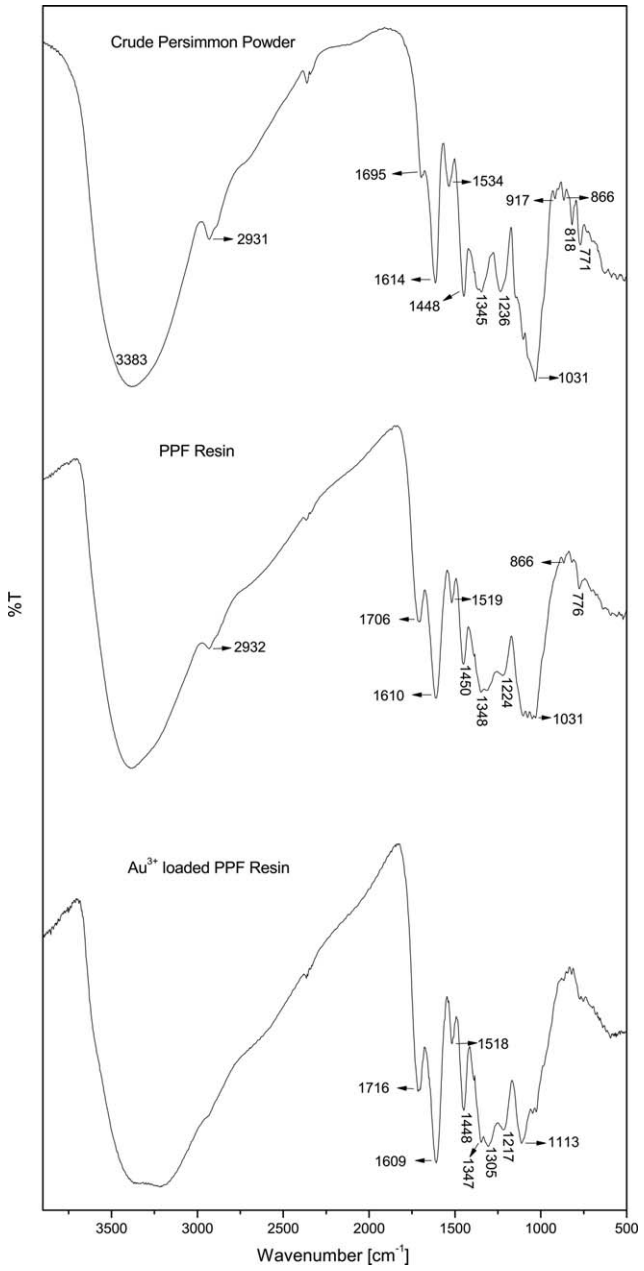

Figure 2. FTIR spectrum of crude persimmon powder and the PPF resin (before and after adsorption of Au^{3+}).

of 1 cm inner diameter and 20 cm high. Approximately 100 mg of PPF resin was packed into the column. Prior to passing the test solution, the column was conditioned by passing deionized water (pH 2.0) for 24 h. Then 150 mg L^{-1} Au^{3+} solution (pH 2.0) was fed at a constant flow rate of 6 mL h^{-1} through the column using a peristaltic pump (DHL-A, China). The effluent solution was collected at 1 h time intervals using a fraction collector (BSZ-100, China) to measure the corresponding metal ion concentrations.

To elute the adsorbed metal ions, the loaded column was prewashed with deionized water (pH 2.0) for 24 h so as to expel any unbound metal ions and then 1 mol L^{-1} thiourea solution (pH 2.0) was passed through the column at identical rate (6 mL h^{-1}). The eluate was collected at each half-hour interval of time for measuring the metal concentration.

Instrumentation Analyses

Metal ion concentrations in the aqueous solutions were measured by atomic absorption spectrophotometer (AAS, Varian Spectra AA 220). The FT-IR spectra of the feed material as well as the adsorbent (before and after adsorption of Au^{3+}) were recorded by a Fourier transform infrared (FTIR) spectrophotometer using KBr pellet method (Thermo FTIR-330). Zeta potentials of PPF resin were measured over the pH range of 2.0-10.0 on a zetasizer (Malvern ZEN 3600). The surface area of PPF resin was determined using the Btunaure-Emmet-Teller method by autosorb-1 standard physical adsorption analyzer (Quantachrome Autosorb-1 JEDL-6390/LV). The thermal denaturation temperature of PPF resin was determined using a differential scanning calorimeter (NETZSCH DSC 204 F1). The X-ray diffraction (XRD) pattern and digital micrograph image of adsorbents after adsorption were recorded by using X-ray diffractometer (Bruker D8 advance) and microscope (Olympus BX61). Surface morphology of PPF resin, before and after adsorption of Au^{3+}, was examined in a scanning electron microscope (SEM, JEOL JSM-6390LV).

RESULTS AND DISCUSSION

Characterization of the Adsorbent

Characterization of crude persimmon powder and the adsorbent (before and after adsorption of Au^{3+}) was investigated by FTIR spectra, the results of which are shown in Figure 2. In the FTIR spectrum of crude persimmon powder, the characteristic broad band at 3383 cm^{-1} is attributed to O—H stretching vibration, the weak band at 1695 cm^{-1} and the sharp band at 1614 cm^{-1} are attributed to C=O stretching vibrations of ester and ketone groups, the bands at 1534 and 1448 cm^{-1} are due to ring C—C stretching vibrations, and the peaks at 1345, 1236, and 1031 cm^{-1} are attributed to O—H bending, C=C—O stretching and C—O—C stretching vibrations, respectively.[24,25] The small peak at 2931 cm^{-1} is attributed to C—H stretching of phenolic rings and the methylene (—CH_2—) bridges formed by the reaction between persimmon tannin and formaldehyde, and the peaks at the region of 910–740 cm^{-1} can be attributed to the deformation vibrations at C—H bond in the phenolic rings.[26] After crosslinking, intensity of O—H stretching vibrations was slightly decreased, inferring that crosslinking has taken place through the condensation reaction of phenolic hydroxyl groups, and the bands at 1706, 1610, and 1224 cm^{-1} due to C=O stretching and C=C—O stretching vibrations were broadened and appeared as moderate bands probably due to partial oxidation of phenolic hydroxyl groups to quinone groups.[24] The intensity of 910-740 cm^{-1} was decreased, inferring that persimmon tannin was highly crosslinked with formaldehyde. In the FTIR spectrum after gold adsorption, the intensity of the band around 1710 cm^{-1} assigned for quinine type C=O stretching was increased. This result suggests that the hydroxyl groups (O—H) of PPF resin particles were oxidized to carbonyl groups (C=O). The band around 1220 cm^{-1} attributable to C=C—O asymmetrical stretching was also increased in intensity, which support the proposed that oxidation of phenolic hydroxyl

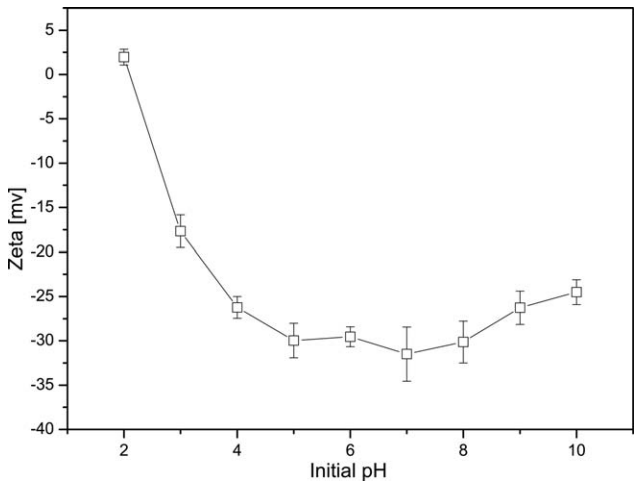

Figure 3. Zeta potentials of PPF resin. (Weight of adsorbent = 10 mg, volume of 0.01 mol L^{-1} NaCl solution = 100 mL, and pH = 2.0-10.0.)

groups has actually taken place, which will be discussed later in detail.

The zeta potentials of PPF resin at different pH values were measured and the results are shown in Figure 3. The isoelectric point of PPF resin occurs at pH 2.21, inferring that the surface will be negative charged above this pH due to the ionization of the functional groups such as adjacent hydroxyl groups. It can be seen that the zeta potentials of PPF resin became more negative as pH increases and exhibited all negative values within the pH range 3.0–10.0, however, the zeta potential was +1.97 mV at pH 2.0.

The bulk density, BET specific surface area, and thermal denaturation temperature of PPF resin were measured as 0.81 g cm^{-3}, 0.23 m^2 g^{-1}, and 367.6 K, respectively.

Effect of pH

Au^{3+} adsorption from aqueous solutions by the PPF resin depended on the solution pH. The effect of pH on adsorption of Au^{3+} by PPF resin is shown in Figure 4. The maximum adsorption occurred at pH 2.0 and adsorption decreased when pH was increased further. In addition, the pH of the solution was observed to be decreased rapidly with adsorption of Au^{3+}. The predominant complex of gold in aqueous chloride solution is $AuCl_4^-$ at pH below 3.0, and increasing solution pH would cause the hydrolysis reaction of $AuCl_4^-$ to proceed that generate hydrolyzed chlorogold complexes such as $AuCl_3(OH)^-$ appear in the aqueous chloride solution.[1] The adjacent hydroxyl groups in B-rings of PT can bind with $AuCl_4^-$ as electron donor in the adsorption reaction. The pH was decreasing rapidly with adsorption of Au^{3+} due to the hydrogen ions that were released from phenolic hydroxyl groups of PT with releasing of electrons in the reductive adsorption process. As pH increases, the adsorbent surface becomes more and more negatively charged, which is shown in Figure 3, and therefore the adsorption of negatively charged chlorogold complexes is rather unfavorable. At pH 2, the surface of PPF resin is positively charged and it is favorable for the attraction of negatively charged metal ions such as $AuCl_4^-$ due to electrostatic interaction. As the feed materials such as e-wastes are leached with strong acid like aqua regia according to the classical method of gold recovery, the PPF resin can be good candidate for gold recovery from this acidic leach liquor.

It is interesting that the filtrates collected from Au^{3+} solutions showed brick red color (initial pH 3.0-4.0) and slate gray color (initial pH 5.0-6.0) as shown in the Supporting Information (Fig. S1), and precipitate generated after remaining static for several hours. By contrast, when the adsorption was conducted at initial pH 2.0, the collected filtrates were colorless, and no precipitation was observed. These results suggested that the adsorption mechanism of Au^{3+} on PPF resin should be varied at different pH range. At pH range of 3.0-6.0, the adjacent hydroxyl groups of PPF resin are ionized, and the Au^{3+} can be firstly chelated with the ionized phenolic hydroxyls and subsequently reduced.[21] However, the ionization of phenolic hydroxyls of PPF resin would be suppressed at low pH range of 2.0-3.0,[29] and the phenolic groups of PPF resin should be protonated and attract the Au^{3+} (exists as $AuCl_4^-$) via electrostatic interaction as mentioned before. At pH range of 3.0-6.0, Au^{3+} was reductively adsorbed on PPF resin, and then the formed elemental Au was partially released into aqueous solutions due to its instability under such pH.[21,29] Hence, it can be inferred that these elemental Au should be in nanoscale because the filtrates were of brick red or slate gray color,[29] and the released nanoscale gold particles were further aggregated to form bigger gold aggregates, thus resulting in the precipitation. On the contrast, no gold adsorbed on PPF resin was released into solution at pH 2.0 possibly due to the formed elemental Au was relatively more stable.

Figure 5 shows the XRD patterns of PPF resin obtained before (a) and after (b) the adsorption of Au^{3+}. As presented in Figure 5(a), the appearance of a broad peak at around 2θ value of 20° indicated the existence of amorphous silica and no elemental Au in the sample. However, it can be observed that the intensive characteristic peaks of elemental Au were located at around 2θ values of 38.2°, 44.4°, 64.6°, and 77.6° from Figure 5(b). The results confirmed that the Au^{3+} could be reduced to elemental Au on the PPF resin during the adsorption. To observe the adsorption

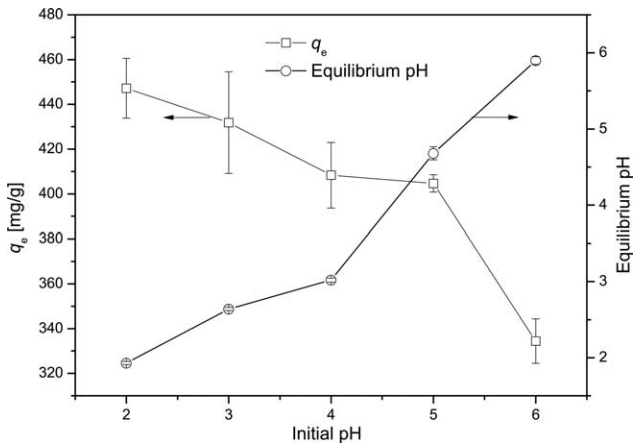

Figure 4. Effect of pH on adsorption of Au^{3+} on PPF resin. (Initial conc. of Au^{3+} = 150 mg L^{-1}, pH = 2.0-6.0, adsorbent dose = 0.3 g L^{-1}, temperature = 303 K, shaking speed = 200 r min^{-1}, and shaking time = 24 h.)

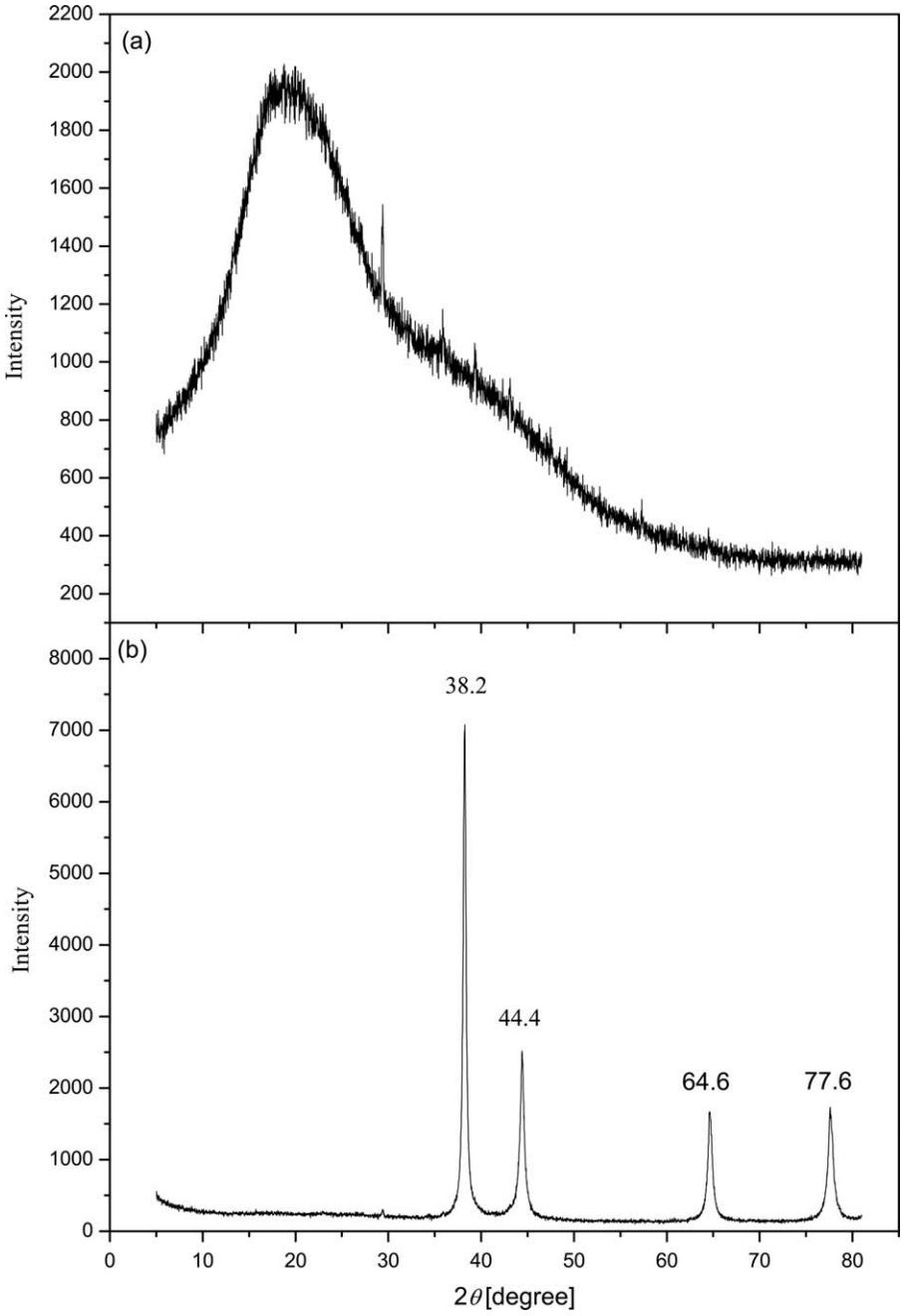

Figure 5. XRD patterns of PPF resin obtained before (a) and after (b) the adsorption of Au^{3+}.

process of Au^{3+} on PPF resin visually, the SEM images and digital micrograph of PPF resin were taken before [Figure 6(a)] and after [Figure 6(b-d)] the adsorption of Au^{3+} as shown in Figure 6. It is clearly visible in Figure 6(b) that the nanoscale gold particles were firstly adsorbed on the surface of PPF resin, and the adsorbed nanoscale gold particles were aggregated to form bigger gold aggregates then separated from resin surface as revealed by Figure 6(c). From Figure 6(d), it is distinct to observe the fine gold particles attached on the PPF resin surface, which further confirmed the formation of elemental Au after the adsorption of Au^{3+}. From the results the adsorption of Au^{3+} on PPF resin may be presumably to be consisted of three steps:[24] (1) binding of anionic species of gold onto positively charged resin surface via electrostatic interaction; (2) reduction of adsorbed Au^{3+} to elemental gold by electron-donor groups (adjacent phenolic hydroxyl groups); (3) aggregation of elemental nanoscale gold particles and formation of bigger gold aggregates.

Adsorption Kinetics

The adsorption kinetics of Au^{3+} on PPF resin is shown in Figure 7(a). It can be observed that the recovery extent of Au^{3+} significantly increased to about 60% in the first 2 h and the adsorption equilibrium could be quickly achieved within 8 h at 303, 313, and 323 K, respectively. The adsorption of Au^{3+} on

Applied Polymer SCIENCE

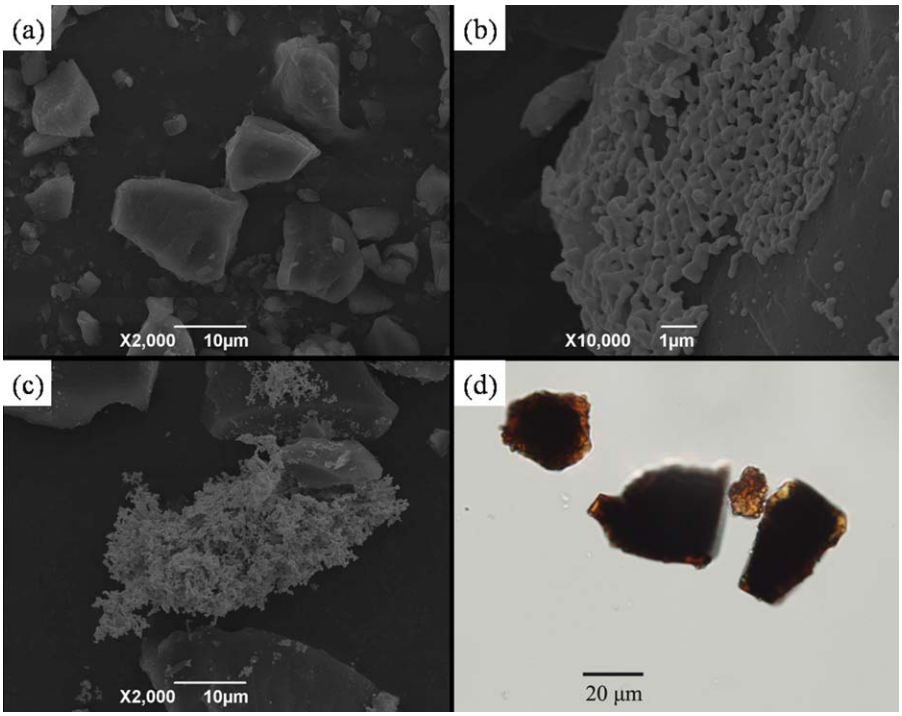

Figure 6. SEM images of PPF resin taken before (a) and after (b, c) the adsorption of Au^{3+} and micrograph of PPF resin taken after (d) the adsorption of Au^{3+}. [Color figure can be viewed in the online issue, which is available at wileyonlinelibrary.com.]

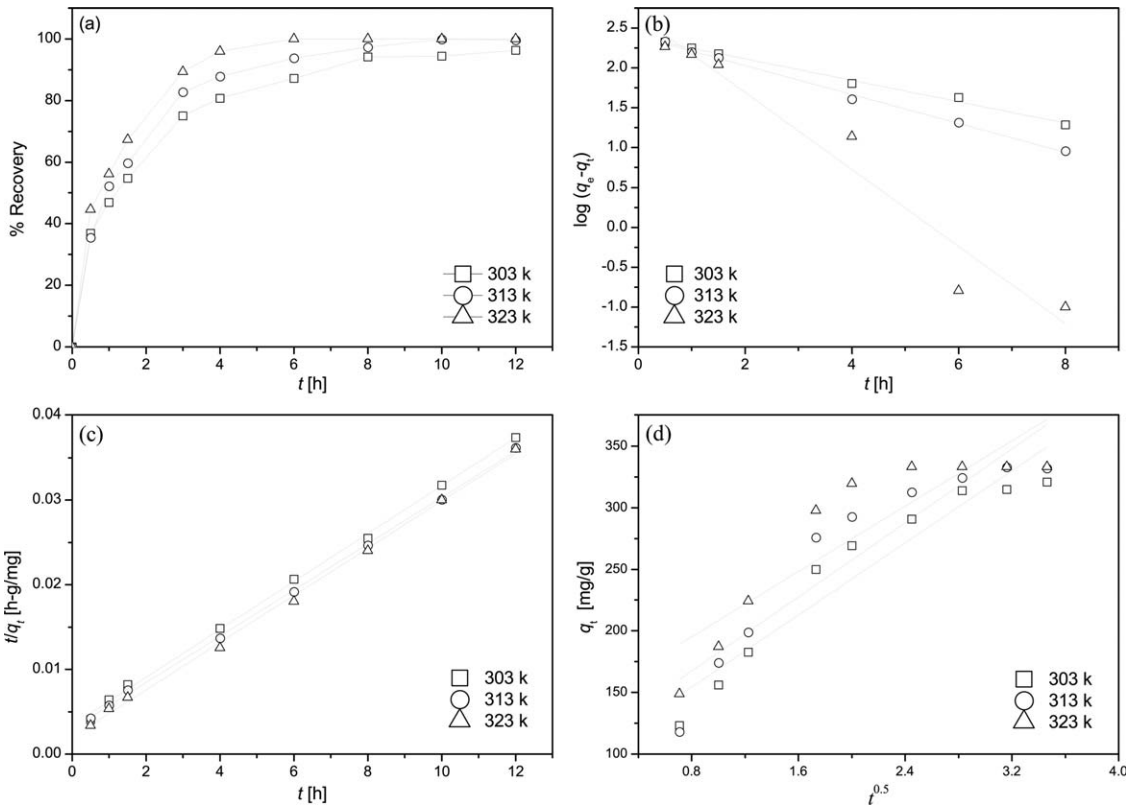

Figure 7. Adsorption kinetics of Au^{3+} on PPF resin. (a) Experimental plots; (b) pseudo-first-order rate model fitting plots; (c) pseudo-second-order rate model fitting plots; (d) intraparticle diffusion model fitting plots. (Initial conc. of Au^{3+} = 100 mg L^{-1}, pH = 2.0, adsorbent dose = 0.3 g L^{-1}, temperature = 303, 313, and 323 K, respectively, shaking speed = 200 r min^{-1} and shaking time = 0.5-12 h.)

Table I. The Adsorption Kinetics Model Parameters of Au^{3+} on PPF Resin

	Pseudo first-order		Pseudo second-order		Intraparticle diffusion	
Temperature (K)	k_1 (h^{-1})	R^2	$k_2 \cdot 10^{-3}$ (g mg^{-1} h^{-1})	R^2	k_{id} (mg g^{-1} $h^{-0.5}$)	R^2
303	0.309	0.993	2.356	0.999	73.154	0.909
313	0.418	0.996	2.501	0.999	75.141	0.852
323	1.112	0.939	3.826	0.998	66.276	0.772

R^2: correlation coefficient.Initial conc. of Au^{3+} = 100 mg L^{-1}, pH = 2.0, adsorbent dose = 0.3 g L^{-1}, temperature = 303, 313, and 323 K, respectively, shaking speed = 200 r min^{-1}, and shaking time = 0.5–12 h.

PPF resin was fast due to little micropore at the outer surface of PPF resin, which suggested that the adsorption of Au^{3+} should take place at the outer surface of PPF resin, and thus the intraparticle diffusion resistance could be neglected.

To confirm our predication, the adsorption kinetic data were further analyzed using the pseudo-first-order rate model,[30] the pseudo-second-order rate model,[31] and the intraparticle diffusion model[32], which are expressed as eqs. (1), (2), and (3), respectively:

$$\log(q_e - q_t) = \log q_e - \frac{k_1 t}{2.303} \quad (1)$$

$$\frac{t}{q_t} = \frac{1}{(q_e)^2 k_2} + \frac{t}{q_e} \quad (2)$$

$$q_t = k_{id} t^{0.5} \quad (3)$$

where q_e and q_t are the amounts of Au^{3+} adsorbed (mg g^{-1}) at equilibrium and at time t (h), respectively, and k_1 (h^{-1}) and k_2 (g mg^{-1} h^{-1}) are the rate constant, k_{id} (mg g^{-1} $h^{-0.5}$) is the intraparticle diffusion rate constant. As shown in Figure 7(b,c), the correlation coefficient (R^2) for the pseudo-first-order rate model and the pseudo-second-order rate model had high values; however, the correlation coefficient R^2 for the intraparticle diffusion model was not satisfactory, as illustrated in Figure 7(d). Meanwhile, values of the calculated q_e from the pseudo-first/second-order rate model were close to those determined by experiments. Both the linearity and the coincidence of the Figure 7(b,c) support the adsorption of Au^{3+} on PPF resin that the first- and/or second-order chemical reaction was a rate-controlled process,[33,34] and the reduction step may be the main rate-determining step. The adsorption kinetics model parameters of Au^{3+} on PPF resin were summarized in Table I.

The relationship between the evaluated pseudo-first-order rate constant and temperature were rearranged according to the Arrhenius equation expressed by the following equation:

$$\ln k = \ln A - \frac{E_a}{RT} \quad (4)$$

where k is rate constant, E_a is activation energy, T is absolute temperature, A is Arrehenius constant, and R is gas constant. The apparent activation energy, E_a, was evaluated as 53.19 kJ mol^{-1}, similar result was observed in the adsorption of gold on wattle tannin gel in the previous work (27.7 kJ mol^{-1}).[1] The positive and very high value of E_a suggested that the adsorption of Au^{3+} on PPF resin was an endothermic chemical phenomenon.

Adsorption Isotherms

Figure 8(a) presents the adsorption isotherms of Au^{3+} on PPF resin. The adsorption capacity was positively correlated to the initial solution concentration and temperature, which supported that the adsorption was an endothermic process as proposed earlier.

Adsorption isothermal data were further analyzed by the Langmuir and Freundlich isotherm models.[35,36] As there was no theoretical model to describe the adsorption isotherms of liquid/solid adsorption, the adsorption isothermal models used in gas/solid adsorption were always used to describe liquid/solid adsorption. The Langmuir isotherm model is based on the assumption of monolayer adsorption on a homogenous surface with identical adsorption sites, its linear form can be expressed by the following equation:

$$\frac{C_e}{q_e} = \frac{C_e}{q_m} + \frac{1}{bq_m} \quad (5)$$

where C_e is the equilibrium concentration of Au^{3+} (mg L^{-1}), q_e is the amount of Au^{3+} adsorbed at equilibrium (mg g^{-1}), q_m is the monolayer adsorption capacity (mg g^{-1}) and b is the Langmuir constant related to the energy of adsorption (L mg^{-1}). The empirical Freundlich model is appropriate for the adsorption on heterogeneous surfaces. The Freundlich isotherm model's linear form is expressed by the following equation:

$$\ln q_e = \ln k_F + \frac{1}{n} \ln C_e \quad (6)$$

where k_F is the Freundlich constant related to the adsorption capacity, and n^{-1} is the heterogeneity factor. An n value between 1 and 10 indicates beneficial adsorption,[37] which represents a heterogeneous surface structure for the adsorbent with an exponential distribution of energy of the surface active-sites.[38] The correlation coefficient (R^2) for the Freundlich model was higher than the Langmuir model, indicating that the adsorption isothermal data were well fitted by the Freundlich equation. In addition, the values of n were 1.53, 1.70, and 1.67 at 293, 303, and 313 K, respectively, which were in the range of 1–10, indicating that the adsorption process can proceed easily. The Langmuir and Freundlich isotherm constants of Au^{3+} on PPF resin were summarized in Table II.

To examine the maximum adsorption capacity for Au^{3+}, 10 mg PPF resin was added into 100 mL Au^{3+} solution (781.20 mg L^{-1}) at initial pH 2.0 and 323 K by shaking for 48 h at a speed of 200 r

Applied Polymer SCIENCE

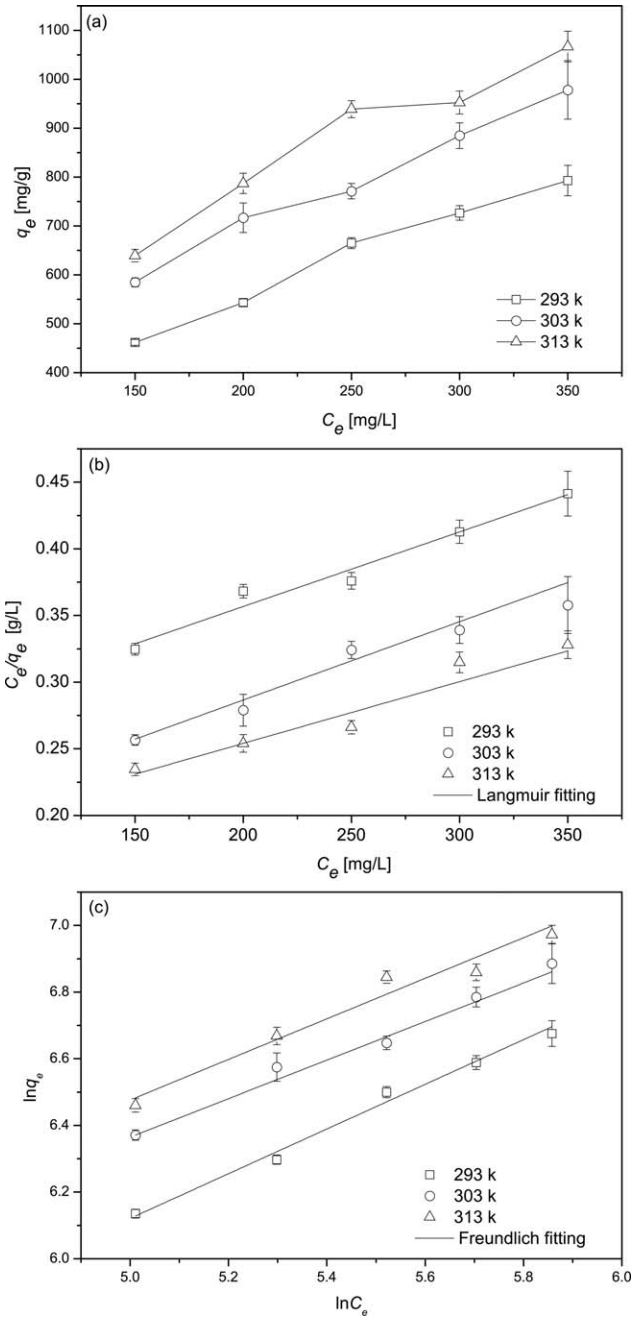

Figure 8. Adsorption isotherms of Au^{3+} on PPF resin. (a) Experimental plots; (b) Langmuir plots; (c) Freundlich plots. (Initial conc. of Au^{3+} = 150-350 mg L^{-1}, pH = 2.0, adsorbent dose = 0.3 g L^{-1}, temperature = 293, 303, and 313 K, respectively, shaking speed = 200 r min^{-1} and shaking time = 24 h.)

min^{-1}. And it was found that the PPF resin had an extremely high adsorption capacity of Au^{3+} (3025.20 mg g^{-1}). The maximum adsorption capacity of PPF resin on the adsorption of Au^{3+} was compared with other biomass materials reported in the literature. As revealed by Table I, the absorbents[1,23–29] prepared from condensed tannin showed much higher adsorption capacity of Au^{3+} than other biomass materials[10,11,13,34,39,40] for condensed tannins have multiple adjacent phenolic hydroxyls and exhibit specific affinity to Au^{3+}. The PPF resin showed better performance on Au^{3+} adsorption compared to most of the biomass materials as presented in Table III.

Column Adsorption and Elution of Au^{3+}

A column experiment for adsorption of Au^{3+} was conducted using the PPF resin. Figure 9(a) shows the breakthrough profiles of Au^{3+} using a column packed with PPF resin. It is apparent that the breakthrough of Au^{3+} took place after 800 B. V. (bed volume), however, adsorption equilibrium was not achieved even after 8,000 B. V. (206.7 h). In the adsorption process, the adsorption zone (also called mass transfer zone, where the bulk of adsorption occurs) moves forward as time passes and then approaches the exit of the bed, and the concentration of the adsorbate at the exit should equal to the concentration in feeding when the adsorption zone is completely moved out through the column.[41] The PPF resin had extremely high adsorption capacity toward Au^{3+} and there was little micropore at the outer surface of PPF resin, indicating that it took a long time for the adsorption zone to approach the exit of the bed. The upper surface layer of bed showed brick red color after the column experiment, which suggested that the loaded Au^{3+} was aggregated at the upper surface layer of bed with the nanoscale gold particles form. Hence, it is quite reasonable to propose that the reduced gold particles were separated from the resin surface leading to the generation of new active sites, which increased the absorbability of the PPF resin, and thus resulting in achieving saturation with difficulty. Figure 9(b) shows the elution profile of the loaded Au^{3+} with acidic thiourea solution. It was found that the loaded Au^{3+} on the column was easily desorbed by acidic thiourea solution (1.0 mol L^{-1}). Furthermore, the regenerated PPF resin could be reused for the adsorption of Au^{3+} with little loss of adsorption capacity.

Recovery of Au^{3+} from An Actual Industrial Sample

An adsorption test was conducted for recovery of Au^{3+} from an actual industrial sample. To examine the selective adsorption capacity for Au^{3+}, 15 mg PPF resin was added into an actual industrial sample (pH 2.0) at 323 K by shaking for 24 h at a speed of 200 r min^{-1}. As shown in Table S1 (as shown in Supporting Information), 100% of Au^{3+} was recovered and the adsorption of Cu^{2+}, Fe^{3+}, Pb^{2+}, and Zn^{2+} was negligible although their concentration was much higher than Au^{3+}.

To elucidate the adsorption mechanism more clearly, it is necessary to investigate the adsorption selectivity of PPF resin to Au^{3+} from aqueous solution with some coexisting metal ions

Table II. Langmuir and Freundlich Isotherm Constants of Au^{3+} on PPF Resin

	Langmuir fitting			Freundlich fitting		
Temperature (K)	q_m (mg/g)	$b \cdot 10^{-3}$	R^2	k_F	n	R^2
293	1798.561	2.269	0.965	17.248	1.525	0.990
303	1904.762	2.917	0.971	30.727	1.697	0.988
313	2096.436	3.000	0.986	32.201	1.665	0.988

R^2: correlation coefficient.Initial conc. of Au^{3+} = 150–350 mg L^{-1}, pH = 2.0, adsorbent dose = 0.3 g L^{-1}, temperature = 293, 303, and 313 K, respectively, shaking speed = 200 r min^{-1}, and shaking time = 24 h.

Table III. Adsorption Capacities (q) of Different Adsorbents Towards Au^{3+}

Adsorbent	q (mg/g)	Conditions	Reference
Wattle tannin gel	8000	pH 2.0, 333 K	1
Dimethylamine modified persimmon waste gel	1109.11	0.1 mol L^{-1} HCl, 303 K	23
Crosslinked persimmon tannin gel	1516.9	0.1 mol L^{-1} HCl, 303 K	24
Bisthiourea modified persimmon tannin gel	1020.46	0.1 mol L^{-1} HCl, 303 K	25
Bayberry tannin-immobilized mesoporous silica	642.0	pH 2.0, 323 K	36
Orange waste gel	1.97	0.1 mol L^{-1} HCl, 303 K	10
Fucus vesiculosus	68.95	pH 7.0, ±296 K	13
Rice husk carbon	149.72	-	11
Chemically modified chitosan	669.8	-	37
Crosslinked chitosan resin	70.34	-	38
Glycine modified crosslinked chitosan resin	169.42	pH 2.0, 333 K	39
PPF resin	3025.20	pH 2.0, 323 K	This work

Initial conc. of Au^{3+} = 781.20 mg L^{-1}, pH = 2.0, adsorbent dose = 0.1 g L^{-1}, temperature = 323 K, shaking speed = 200 r min^{-1}, and shaking time = 48 h.

at varying initial pH. As illustrated in Figure 10, PPF resin exhibited remarkable selectivity for Au^{3+} over the pH range of 1-2, while the adsorption of base metal ions was negligible. However, the adsorption of Fe^{3+} and Pb^{2+} was increasing rapidly with the pH increased from 2.0 to 5.0, while the adsorption of Cu^{2+} and Zn^{2+} was increasing slowly. As mentioned earlier, at pH below 3.0, the predominant complex of Au is $AuCl_4^-$ in acidic aqueous chloride solutions and the PPF resin surface become positively charged due to protonation, and thus anionic species $AuCl_4^-$ can bind onto positively charged resin surface by electrostatic interaction. However, the majority of base metals such as Cu^{2+}, Fe^{3+}, Pb^{2+}, and Zn^{2+} exist as positively charged species in acidic aqueous solutions at pH below 3.0, so the PPF resin exhibited little adsorption capacity to them. The lower accessibility of Cu^{2+} and Zn^{2+} compared with Fe^{3+} and Pb^{2+} is possibly due to their respective ionic volume, in which the metal ions uptake increase as the ionic volume increased. The result verified the PPF resin had outstanding selectivity to Au^{3+}, which suggested the

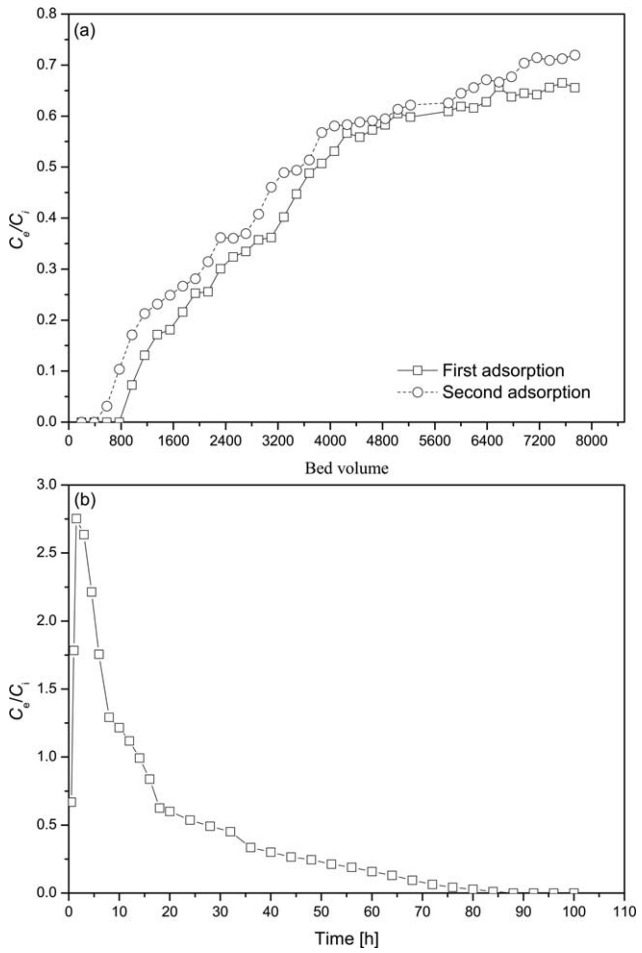

Figure 9. (a) Breakthrough profiles and (b) elution profiles of Au^{3+} on PPF resin. (C_i: initial conc. of Au^{3+} = 150 mg L^{-1}, C_e: conc. of Au^{3+} in effluent, pH = 2.0, weight of adsorbent = 100 mg, temperature = 298 ± 5 K, and flow rate = 6 mL h^{-1}.)

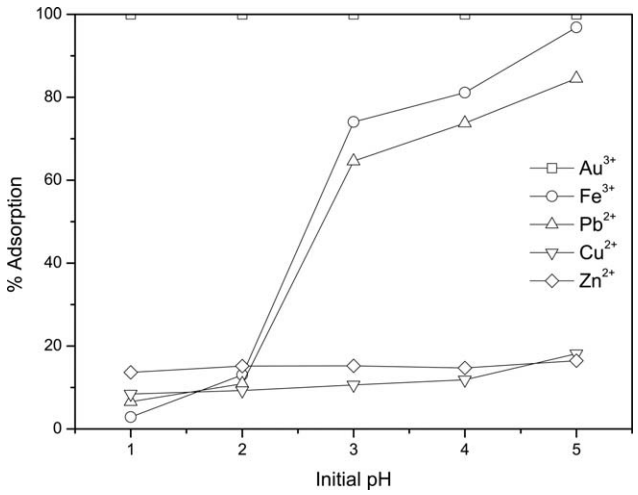

Figure 10. Adsorption behavior of PPF resin for various metal ions at varying initial pH. (Initial metal ion conc. = 100 mg L^{-1}, pH = 1.0-5.0, adsorbent dose = 0.3 g L^{-1}, temperature = 303 K, shaking speed = 200 r min^{-1} and shaking time = 24 h.)

PPF resin could be used for gold recovery in practical application.

CONCLUSIONS

The PPF resin was highly effective and selective for the adsorption recovery of Au^{3+} from acidic aqueous solutions. The PPF resin exhibited a fast adsorption rate to Au^{3+}, and the experimental data were well fitted with the pseudo-first/second-order rate model. As revealed by the high E_a value (53.19 kJ mol^{-1}), adsorption of Au^{3+} on PPF resin was found to be an endothermic process. In addition, the PPF resin showed a high adsorption capacity (3025.20 mg g^{-1}) at 323 K. The adsorption isotherms could be well described by Freundlich equation compared with the Langmuir equation. The adsorption of Au^{3+} on the column packed with PPF resin was effective and the loaded Au^{3+} on the column could be easily desorbed by acidic thiourea solution. Furthermore, the regenerated PPF resin could be reused for the adsorption of Au^{3+} with little loss of adsorption capacity. The adsorption of Au^{3+} on PPF resin was a reductive adsorption process, in which Au^{3+} was reduced to its elemental form and aggregated to fine gold particles. In this context, we have explored the potential utilization of PPF resin as a good candidate for the recovery of Au^{3+} from aqueous environment.

ACKNOWLEDGMENTS

This research was financially supported by Special Fund for Agro-scientific Research in the Public Interest (201203047) and the Fundamental Research Funds for the Central Universities (2009PY024).

REFERENCES

1. Ogata, T.; Nakano, Y. *Water. Res.* **2005**, *39*, 4281.
2. Navarro, P.; Vargas, C.; Alonso, M.; Alguacil, F. *J. Gold Bull.* **2006**, *39*, 93.
3. Ran, Y.; Fu, J. M.; Rate, A. W.; Gilkes, R. J. *Chem. Geol.* **2002**, *185*, 33.
4. Van Nguyen, N.; Lee, J. C.; Kim, S. K.; Jha, M. K.; Chung, K. S.; Jeong, J. *Gold Bull.* **2010**, *43*, 200.
5. Aktas, S.; Morcali, M. H. *Int. J. Miner. Process.* **2011**, *101*, 63.
6. Firlak, M.; Kahraman, M. V.; Yetimoglu, E. K. *J. Appl. Polym. Sci.* **2012**, *126*, 322.
7. Nabid, M. R.; Sedghi, R.; Hajimirza, R.; Oskooie, H. A.; Heravi, M. M. *Microchim. Acta* **2011**, *175*, 315.
8. Lim, J. S.; Kim, S. M.; Lee, S. Y.; Stach, E. A.; Culver, J. N.; Harris, M. T. *J. Colloid Interface Sci.* **2010**, *342*, 455.
9. Kenney, J. P. L.; Song, Z.; Bunker, B. A.; Fein, J. B. *Geochim. Cosmochim. Acta* **2012**, *87*, 51.
10. Kawakita, H.; Abe, M.; Inoue, J.; Ohto, K.; Harada, H.; Inoue, K. *Sep. Sci. Technol.* **2009**, *44*, 2797.
11. Chand, R.; Wateri, T.; Inoue, K.; Kawakita, H.; Luitel, H. N.; Parajuli, D.; Torikai, T.; Yada, M. *Miner. Eng.* **2009**, *22*, 1277.
12. Chen, X. Q.; Lam, K. F.; Mak, S. F.; Yeung, K. L. *J. Hazard. Mater.* **2011**, *186*, 902.
13. Mata, Y. N.; Torres, E.; Blázquez, M. L.; Ballester, A.; González, F. and Muñoz, J. *J. Hazard. Mater.* **2009**, *166*, 612.
14. Vijayaraghavan, K.; Mahadevan, A.; Sathishkumar, M.; Pavagadhi, S.; Balasubramanian, R. *Chem. Eng. J.* **2011**, *167*, 223.
15. Bratskaya, S. Y.; Ustinov, A. Y.; Azarova, Y. A.; Pestov, A. V. *Carbohydr. Polym.* **2011**, *85*, 854.
16. Pangeni, B.; Paudyal, H.; Abe, M.; Inoue, K.; Kawakita, H.; Ohto, K.; Adhikari, B. B.; Alam, S. *Green Chem.* **2012**, *14*, 1917.
17. Pangeni, B.; Paudyal, H.; Inoue, K.; Kawakita, H.; Ohto, K.; Alam, S. *Cellulose* **2012**, *19*, 381.
18. Matsuo, T.; Ito, S. *Agric. Biol. Chem.* **1978**, *42*, 1637.
19. Liao, X. P.; Li, L.; Shi, B. J. *Radioanal. Nucl. Chem.* **2004**, *260*, 619.
20. Nakajima, A.; Ohe, K.; Baba, Y.; Kijima, T. *Anal. Chem.* **2003**, *19*, 1075.
21. Parajuli, D.; Kawakita, H.; Inoue, K.; Ohto, K.; Kajiyama, K. *Hydrometallurgy* **2007**, *87*, 133.
22. Kawakita, H.; Yamauchi, R.; Parajuli, D.; Ohto, K.; Harada, H.; Inoue, K. *Sep. Sci. Technol.* **2008**, *43*, 2375.
23. Xiong, Y.; Adhikari, C. R.; Kawakita, H.; Ohto, K.; Inoue, K.; Harada, H. *Bioresour. Technol.* **2009**, *100*, 4083.
24. Gurung, M.; Adhikari, B. B.; Kawakita, H.; Ohto, K.; Inoue, K.; Alam, S. *Chem. Eng. J.* **2011**, *174*, 556.
25. Gurung, M.; Adhikari, B. B.; Kawakita, H.; Ohto, K.; Inoue, K.; Alam, S. *Ind. Eng. Chem. Res.* **2012**, *51*, 11901.
26. Oo, C. W.; Kassim, M. J.; Pizzi, A. *Ind. Crops Prod.* **2009**, *30*, 152.
27. Oshida, M. K.; Yonemori, K.; Sugiura, A. *Postharvest Biol. Technol.* **1996**, *8*, 317.
28. Nakano, Y.; Takeshita, K.; Tsutsumi, T. *Water Res.* **2001**, *35*, 496.
29. Huang, X.; Wang, Y. P.; Liao, X. P.; Shi, B. *J. Hazard. Mater.* **2010**, *183*, 793.
30. Özacar, M.; Şengil, İ. *Process Biochem.* **2005**, *40*, 565.
31. Ho, Y. S.; McKay, G. *Process Biochem.* **1999**, *34*, 451.
32. Lazaridis, N. K.; Karapantsios, T. D.; Georgantas, D. *Water Res.* **2003**, *37*, 3023.
33. Turse, R.; Rieman, W. III *J. Phys. Chem.* **1961**, *65*, 1821.
34. Donia, A. M.; Atia, A. A.; Elwakeel, K. Z. *Hydrometallurgy* **2007**, *87*, 197.
35. Langmuir, I. *J. Am. Chem. Soc.* **1916**, *38*, 2221.
36. Freundlich H. M. F. Z. *Phys. Chem.* **1906**, *57*, 385.
37. Hall K. R.; Eagleton, L. C.; Acrivos, A.; Vermeulen, T. *Ind. Eng. Chem. Fundam.* **1966**, *5*, 212.
38. Mishra, S. P.; Tiwari, D.; Dubey, R. S.; Mishra, M. *Bioresour. Technol.* **1998**, *63*, 1.
39. Fujiwara, K.; Ramesh, A.; Maki, T.; Hasegawa, H.; Ueda, K. *J. Hazard. Mater.* **2007**, *146*, 39.
40. Ramesh, A.; Hasegawa, H.; Sugimoto, W.; Maki, T.; Ueda, K. *Bioresour. Technol.* **2008**, *99*, 3801.
41. Sun, X.; Huang, X.; Liao, X. P.; Shi, B. *J. Hazard. Mater.* **2010**, *179*, 295.